

Petrogenesis of convergent-margin calc-alkaline rocks and the significance of the low oxygen isotope ratios: the Rodna-Bârgău Neogene subvolcanic area (Eastern Carpathians)

DELIA CRISTINA PAPP^{1*}, IONEL URECHE¹, IOAN SEGHEDI², HILARY DOWNES³ and LUIGI DALLAI⁴

¹Geological Institute of Romania, Cluj-Napoca Branch, P.O. Box 181, 400750 Cluj-Napoca, Romania; deliapapp@pcnet.ro

²Institute of Geodynamics, Str. Jean-Luis Calderon 19–21, 70201 Bucharest, Romania

³Birkbeck/UCL Research School of Geological and Geophysical Sciences, Birkbeck College, Malet St., London WC1E 7HX, United Kingdom

^{4**}Istituto di Geologia Ambientale e Geoingegneria IGAG, c/o Dipartimento Scienze della Terra, Università di Roma “La Sapienza”, P.le Aldo Moro 5, 00185 Rome, Italy

*Present address: CNR—Istituto di Geoscienze e Georisorse, Area di Ricerca di Pisa, Via Moruzzi 1, 56127 Pisa, Italy

(Manuscript received March 28, 2003; accepted in revised form March 16, 2004)

Abstract: Neogene calc-alkaline magmatites (from basaltic andesites to rhyolites including mafic cognate enclaves) of the Rodna-Bârgău subvolcanic area (East Carpathian arc) are evaluated on the basis of new mineral compositional data, major and trace elements, as well as Sr and O isotope data. Two different series of rocks have been separated. The magmas of the medium-K series had a rapid ascent toward the surface, as proven by the presence of primary garnet bearing rocks, or by the sporadic occurrence of mafic cognate enclaves. The $\delta^{18}\text{O}$ values of amphiboles vary from 4.2 to 5.4 ‰ (SMOW). The $\delta^{18}\text{O}$ value measured on garnet is 4.3 ‰. The range of $^{87}\text{Sr}/^{86}\text{Sr}$ ratios is from 0.70588 to 0.70887. The decrease of the $\delta^{18}\text{O}$ values as $^{87}\text{Sr}/^{86}\text{Sr}$ ratios and SiO_2 increase is interpreted as a progressive contamination of a mantle derived magma with a contaminant depleted in $\delta^{18}\text{O}$ and enriched in $^{87}\text{Sr}/^{86}\text{Sr}$ (i.e. hydrothermally altered lower crustal rocks). Within the high-K series the presence of intermediate magma chambers where assimilation-fractional crystallization processes took place is considered. The $\delta^{18}\text{O}$ values measured on clinopyroxenes vary from 4.6 to 5.7 ‰ and on amphiboles from 3.8 to 6.7 ‰. The range of $^{87}\text{Sr}/^{86}\text{Sr}$ ratios is from 0.70605 to 0.70950. The covariation of the $\delta^{18}\text{O}$ values and $^{87}\text{Sr}/^{86}\text{Sr}$ ratios is scattered. The highest $\delta^{18}\text{O}$ values correspond to the highest $^{87}\text{Sr}/^{86}\text{Sr}$ ratios and are consistent with assimilation of the local upper-crustal rocks. The lower $\delta^{18}\text{O}$ values and the observed oxygen isotope disequilibrium between coexisting pyroxenes and amphiboles are explained by interaction with heated meteoric water.

Key words: Eastern Carpathians, subvolcanic intrusions, calc-alkaline magmas, crustal interaction, enclaves, low $\delta^{18}\text{O}$.

Introduction

Neogene magmatic rocks of the Inner Carpathian arc have been the subject of many recent studies (e.g. Salters 1988; Downes et al. 1995; Mason et al. 1996, 1998; Seghedi et al. 1995, 2001). However, there are as yet few published data on the subvolcanic zone in the East Carpathian arc (e.g. Ureche et al. 1995; Papp 1999; Nițoi et al. 2002). Here we report the first detailed geochemical and isotopic study on Neogene magmatic rocks from the Rodna-Bârgău Mountains (Romania), which form the main area of the subvolcanic zone. We evaluate the calc-alkaline magmatism on the basis of new mineral compositional data, major and trace elements, as well as Sr and O isotope data. The role of the mantle source, crustal assimilation and magma mixing is addressed. Parental magmas showing a depleted oxygen isotope signature relative to average MORB are a special feature of the magmatic rocks from the Rodna-Bârgău Mountains. They are interpreted in terms of as-

similation of hydrothermally altered crustal rocks and interaction between intrusive bodies and heated meteoric water.

Up to now, similar low $\delta^{18}\text{O}$ rocks have not been reported within the Carpathian Neogene volcanic arc. More extended occurrences of rocks (e.g. alkaline basalts, granulite enclaves) depleted in oxygen isotope have been described in the Pannonian Basin (e.g. Kempton et al. 1997; Dobosi et al. 2003), but those are related to the distensional efforts behind the Carpathian arc.

Worldwide, significantly ^{18}O -depleted primary magmas have been recovered from plume derived basalts erupted in ocean island settings (e.g. Iceland, Hawaii, Canary Islands) (Eiler 2001 and literature therein). The origin of this low $\delta^{18}\text{O}$ signature has been attributed to either interaction of basaltic magmas within the hydrothermally-altered lower oceanic crust or as a primary feature of the plume itself. For the more evolved magmas from Canary Islands, Thirlwall et al. (1997) favour an interpretation that their ^{18}O -depleted character might have been acquired during contamination by hydrothermally altered rocks in the current lithosphere.

Our study brings new arguments in the debate of the origin of the ^{18}O -depleted magmas enforcing the importance of con-

*Corresponding author: E-mail: deliapapp@pcnet.ro; Tel./Fax: +40264-429430

tamination by hydrothermally altered crustal rocks in continental arc-related magmatism. It also provides new data, which might contribute to improving the models of geotectonic evolution of the Inter-Carpathian area.

Geological setting of the Rodna-Bârgău Mountains

Magmatic rocks in the Inner Carpathian arc are considered by most authors (e.g. Csontos 1995; Balintoni 1996) to belong to an active continental margin, connected to a subduction zone located at the southwestern border of the Eurasian plate. Although subduction was related to Alpine tectonic activity, which started during the Cretaceous, the major convergent event occurred in Miocene times (Săndulescu 1984). Neogene magmatism was associated with the consumption of a small piece of ocean crust, attached to the European plate, beneath the ALCAPA (Alpine-Carpathian-Pannonian) and Tisia-Getia continental blocks (Rădulescu & Săndulescu 1976; Seghedi et al. 1998).

The subvolcanic zone is located on the Tisia-Getia block close to the boundary with both the ALCAPA block and the Eastern European Plate, between the two volcanic segments: Oaş-Gutâi in the north-west and Călimani-Gurghiu-Harghita in the south-east (Fig. 1, insertion). Within the subvolcanic zone numerous intrusive bodies are located in three areas: Țibleș, Toroioaga and Rodna-Bârgău.

In the Rodna-Bârgău area special geological-structural conditions resulted from the tectonic contact of the Rodna metamorphic massif with the Transcarpathian Flysch Zone, delineated by the Someș Fault system (Fig. 1). The host-rocks of the magmatites are crystalline schists of the Middle Dacides and sedimentary deposits of the Transcarpathian flysch.

The intrusive bodies from the Rodna Mountains, hosted by metamorphic rocks, are mostly large massive bodies (stocks, and laccoliths associated with sills and dykes). More acidic facies are represented by: Parva rhyolites, Cormaia rhyodacites and Valea Vinului quartz andesites (porphyritic microgranodiorites). In contrast, sedimentary flysch deposits form the host-rocks of the intrusive bodies in the Bârgău Mountains. The main intrusive units are: Bucnitori and Sturzii (dacites), Pleșii-Mal (quartz garnet andesites), Cornii (andesites), Chicera and Arsente (Măguri) (microdiorites) and Heniu, Oala, Iliuța, Colibița (South Bârgău) (andesites). The intrusions vary in volume and have a surface exposure from 1 km² (Pleșii-Mal) to 20 km² (Cornii, Heniu).

Within the Rodna-Bârgău area the age of the magmatites is 11–9 Ma, corresponding to Pannonian, similar to other volcanic activity in the Eastern Carpathians (Pécskay et al. 1995). The distribution of ages among the delimited intrusive units is as follows: Sturzii 10.6±0.7 Ma, Runc 10.4±0.8 Ma, Valea Vinului 9.0±0.5 Ma, Cornii 9.8±0.8 Ma, Măgura Arsente 8.8±0.5 Ma, and Măgura Rodnei 8.6±0.4 Ma.

Petrography of the magmatites

The main petrographic types of the Neogene magmatites are basaltic andesites, microdiorites, quartz biotite amphibole

andesites, quartz-garnet andesites, dacites, rhyodacites, and rhyolites. Transitional textures occur between subvolcanic and plutonic facies, and between hypabyssal and volcanic-like facies. There is a relatively high degree of crystallization and most of the rocks are porphyritic.

The main minerals are: plagioclase feldspars, amphiboles, pyroxenes, biotite, quartz and subordinate potassic feldspars. The accessory minerals are: apatite, magnetite, zircon, garnet and the secondary minerals are: clay minerals, sericite, chlorite, calcite, and epidote.

Magmatic cognate enclaves are relatively frequent in andesites, microdiorites and diorites (Nițoi et al. 1995). They are subangular to rounded in shape and vary from 2–3 cm up to 20–25 cm in size. The cognate enclaves have a holocrystalline hypidiomorphic structure, frequently showing a poikilitic character due to the presence of large amphibole crystals (megacrystals), which may include other minerals such as pyroxenes and feldspars. The texture is massive. Amphiboles ± feldspars represent the mineralogical composition of most cognate enclaves, forming a hornblende-like composition. Pyroxene ± amphibole ± feldspars (pyroxenite-like) are also present. Within the Valea Vinului quartz andesites, cognate enclaves containing biotite + amphibole + feldspar occur. The contact between cognate enclaves and host-rocks is either sharp or can show evidence of partial dissemination in the host melt. Detailed petrographic descriptions of cognate enclaves and their relationship with the host-rocks can be found in Nițoi et al. (2002).

The magmas that generated the host-rocks in the Rodna-Bârgău Mountains had a calc-alkaline character and show a complete differentiation trend, while the cognate enclaves are much richer in FeO and MgO and display tholeiitic features (Ureche 2000).

Sampling and analytical techniques

We have studied most of the important intrusive rocks in the Rodna-Bârgău sector. Samples of basaltic andesites, microdiorites, quartz biotite amphibole andesites, quartz garnet andesites, dacites, rhyodacites and rhyolites, as well as mafic cognate enclaves, were selected for whole rock and mineral separates analysis.

For most of the whole-rock samples, major elements were determined by wet chemical methods at the Prospecțiuni S.A. (Bucharest) Laboratory. Trace elements and REE have been determined by neutron activation method at the Geological Institute of Romania. In addition, 23 pressed powder pellets from the same whole-rock samples were made for determining Rb, Sr, Y, Zr, Nb content by XRF analyses. For four samples (I4/A2, I4/A3, I4px0, I4px4) complete chemical analysis (major and trace elements) was performed by XRF. XRF analyses have been carried out at the Department of Earth Science of the “La Sapienza” University of Rome, using a PHILIPS 1480 Spectrometer equipped with a Rh tube running at 30 Kv–60 Ma for major elements and 50 Kv–50 Ma for trace elements. Ba, La, Ce, Cr, and V have been performed by a W tube running at 50 Kv–50 Ma conditions. International standards were used for calibration and the precision and accuracy

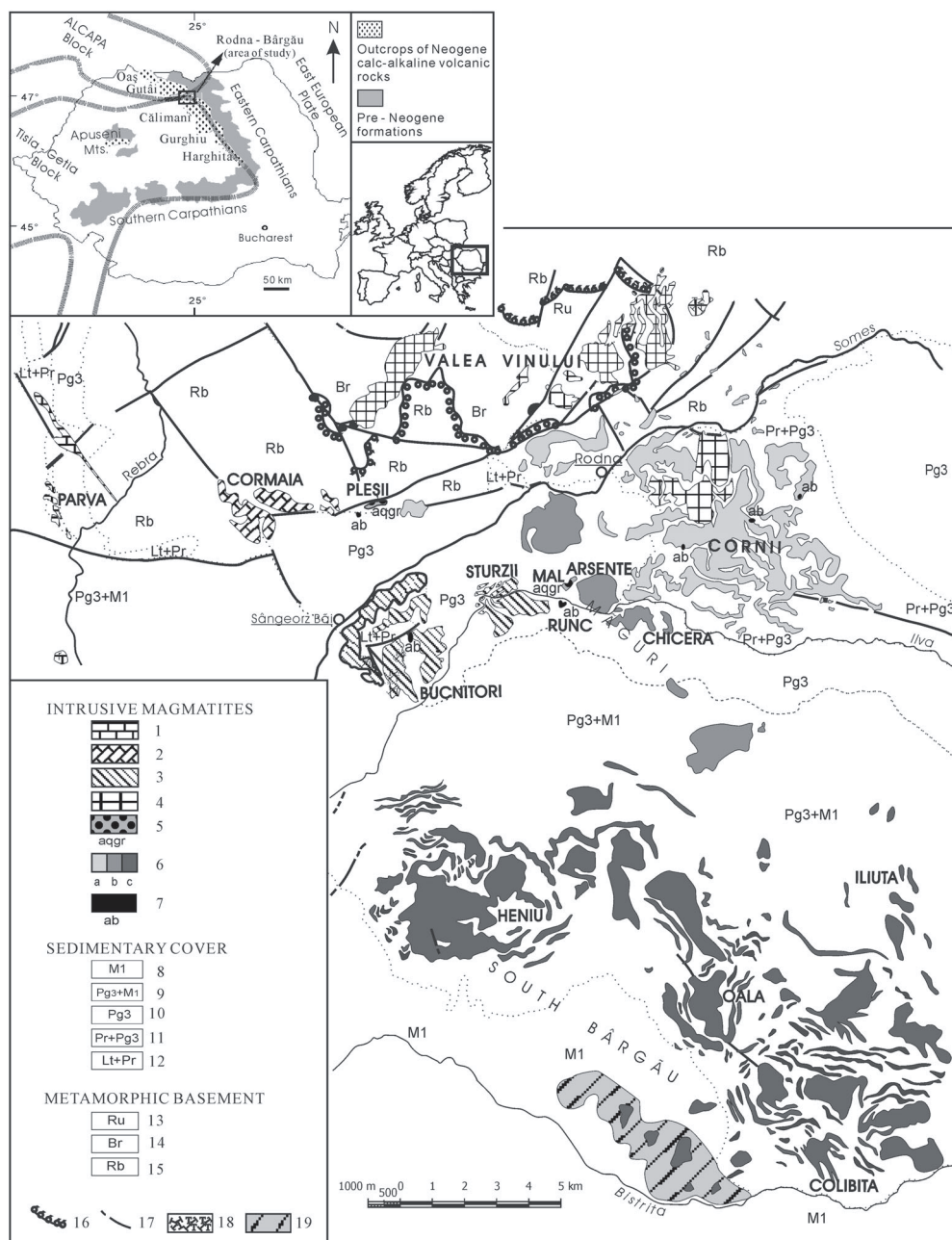


Fig. 1. Geological sketch map of the Rodna-Bârgău Mountains. **Intrusive magmatites (Pannonian):** 1 — rhyolites; 2 — rhyo-dacites; 3 — dacites; 4 — quartz andesites ± biotite; 5 — quartz garnet andesites; 6 — andesites, a — microdiorites, b — diorites, c — (hornblende ± pyroxene); 7 — basaltic andesites. **Sedimentary cover:** 8 — shales, sandstones, pyroclastites (Lower Miocene); 9 — sandstones (Borșa Formation) (Paleogene-Lower Miocene); 10 — shales, sandstones (Paleogene); 11 — marls, shales, breccias (Priabonian-Paleogene); 12 — limestones, sandstones, conglomerates (Lutetian-Priabonian). **Metamorphic basement:** 13 — Rusaia metamorphic series (Silurian); 14 — Rebra metamorphic series (Upper Proterozoic); 15 — Bretila metamorphic series (Upper Proterozoic); 16 — shear zone; 17 — fault; 18 — breccias; 19 — pyroclastic products (Neogene).

for major elements are estimated to be below 3 %. The analytical precision is better than 5 % for Rb, Sr and Y and better than 10 % for other trace elements except for La and Ce, which may be even more than 20 %.

The microprobe analyses were performed on polished thin sections prepared within the laboratory of the CNR — Centro di Studio per il Quaternario e l'Evoluzione Ambientale, Rome (at present Istituto di Geologia Ambientale e Geoingegneria).

The analyses were made using a CAMECA SX50 equipped with 5 WDS spectrometers and one EDS Link eXL. Over 400 points distributed on profiles were measured on amphibole, pyroxene, biotite, feldspar and garnet crystals.

Whole-rock powder samples of host rocks and cognate enclaves were prepared for Sr isotope analyses. The isotope analyses were carried out at the CNR — Centro di Studio per il Quaternario e l'Evoluzione Ambientale, Rome. All samples

were analysed in bulk, and the rocks were decomposed with a mixture of ultrapure HF and HNO₃ in a teflon vessel at 70 °C for 48 h. The resulting solution was evaporated and taken up in 6.2 N ultrapure HCl. The Sr was separated in a 3 ml AG 50W-X8 resin column. Isotopic analyses were carried out using both Finnigan Mat 262RPQ multicollector and VG 54E single collector mass spectrometers. For the latter machine, the procedures of Ludwig (1994) were applied for data acquisition and reduction. Internal precision (within-run precision) of a single analytical result is given as two standard error of the mean. Repeated analyses of standard NBS987 gave averages and errors expressed as 2 standard deviation as follows $^{87}\text{Sr}/^{86}\text{Sr}=0.71024 \pm 2$ (n=20) and the isotope ratios were normalized to $^{86}\text{Sr}/^{88}\text{Sr}$ to 0.1194.

Mineral separates of amphibole, pyroxene and garnet have been analysed for O isotope ratios. Mineral separates were made by hand picking under a microscope. In some cases supplementary purification of the separates was performed, by washing in an ultrasonic bath and/or acetone. Oxygen isotope analyses were carried out at the CNR — Centro di Studio per il Quaternario e l'Evolutione Ambientale, Rome, using a laser fluorination system attached to a Finnigan MAT "DELTA plus" mass spectrometer. Some samples have been replicated or newly performed at the Royal Holloway University of London using a laser fluorination system following the method de-

scribed by Mathey & Macpherson (1993). The determinations made in Italy and the UK are comparable. Two or more extractions were made on each sample; the average reproducibility of isotopic analyses is $\pm 0.2\text{‰}$ or better. The analytical data are reported in the δ -notation referenced to SMOW as the mean of two or more replicate analyses.

Results

Main mineral species

Amphiboles are the main mafic minerals within the magmatic rocks in the Rodna-Bârgău area. All are Ca-rich and have been classified according to IMA (Leake et al. 1997) nomenclature (Table 1). The magnesium number [$Mg\# = MgO / (MgO + FeO)$] varies from 0.53 (Valea Vinului cognate enclave) up to 0.87 (amphibole megacrystal-Arsente cognate enclave). Most amphibole phenocrysts, especially those found in andesites and microdiorites are magnesiohastingsites. Amphiboles from more acidic facies are tschermakites. Amphiboles in cognate enclaves are also relatively heterogeneous, displaying magnesiohastingsite (Chicera-Arsente), pargasite (Cornii) and tschermakite (Heniu) compositions. Zoning is present within most of the amphibole crystals, both in host-

Table 1: Representative microprobe analyses of amphiboles of host rocks and enclaves. Abbreviations: **Hen** — Heniui; **V.Vin** — V.Vinului; **Chi** — Chicera; **Ars** — Arsente; **ro** — rock; **en** — enclave; **r** — rim; **c** — core; **pt** — potassian; **tsch** — tschermakite; **mghas** — magnesiohastingsite; **parg** — pargasite.

Sample Anls. Loc.	I15 ro(r) Sturzii	I15 ro(c) Sturzii	I31 ro Pleșii	I8 ro Hen	I8 en Hen	I18 ro Iliuța	I11 ro V.Vin	I11 ro V.Vin	I5 ro Chi	I5 en Chi	I4 ro Ars	I4 en(r) Ars	I4 en(c) Ars	I4mega en Ars	I14 ro Cornii	I14 en Cornii
SiO ₂	44.53	41.98	41.90	43.06	42.72	43.37	40.95	40.72	42.44	42.70	42.08	41.52	42.64	42.73	42.95	43.27
TiO ₂	0.91	1.00	0.69	1.05	1.86	2.18	1.47	1.83	1.30	1.21	1.67	1.87	1.46	1.19	1.95	2.15
Al ₂ O ₃	11.48	13.98	13.40	11.74	12.18	12.49	12.02	12.69	13.18	13.04	13.13	12.98	13.27	13.12	12.25	11.70
Cr ₂ O ₃	0.00	0.05	0.07	0.03	0.06	0.00	0.08	0.04	0.06	0.06	0.09	0.10	0.08	0.00	0.00	0.10
FeO*	15.96	16.82	17.99	17.51	13.83	14.32	18.69	16.25	9.54	8.86	11.52	13.51	9.52	10.56	12.11	11.50
MnO	0.62	0.51	0.51	0.60	0.23	0.25	0.56	0.35	0.10	0.16	0.23	0.32	0.15	0.15	0.28	0.20
MgO	12.18	10.50	10.33	11.37	12.61	12.75	9.25	10.69	15.28	15.79	14.13	12.68	15.58	15.16	12.77	13.85
CaO	9.78	10.37	9.88	9.56	11.12	10.19	11.35	11.21	11.68	11.73	11.74	11.56	11.92	11.51	11.37	11.92
Na ₂ O	1.40	1.62	1.86	1.70	1.86	2.24	1.46	1.87	2.26	2.22	2.37	2.24	2.49	2.29	2.20	1.96
K ₂ O	0.23	0.32	0.38	0.24	0.48	0.38	1.38	1.38	0.84	0.84	0.75	0.71	0.80	0.69	0.92	0.74
BaO	0.00	0.00	0.01	0.00	0.01	0.00	0.02	0.03	0.03	0.01	0.01	0.00	0.02	0.01	0.01	0.02
F	0.08	0.13	0.14	0.12	0.12	0.00	0.11	0.14	0.21	0.24	0.14	0.08	0.08	0.06	0.21	0.21
Total	97.17	97.27	97.15	96.98	97.08	97.17	97.34	97.19	96.91	96.85	97.84	97.57	98.01	97.47	97.01	97.62
Si	6.51	6.18	6.21	6.35	6.29	6.21	6.21	6.15	6.18	6.20	6.13	6.12	6.14	6.18	6.35	6.34
Al ^{IV}	1.49	1.82	1.79	1.65	1.71	1.79	1.79	1.85	1.82	1.80	1.87	1.88	1.86	1.82	1.65	1.66
T sites	8.00	8.00	8.00	8.00	8.00	8.00	8.00	8.00	8.00	8.00	8.00	8.00	8.00	8.00	8.00	8.00
Al ^{VI}	0.50	0.61	0.55	0.39	0.40	0.37	0.36	0.40	0.44	0.43	0.38	0.37	0.39	0.41	0.49	0.36
Ti	0.10	0.11	0.08	0.12	0.21	0.24	0.17	0.21	0.14	0.13	0.18	0.21	0.16	0.13	0.22	0.24
Cr	0.00	0.01	0.01	0.00	0.01	0.00	0.01	0.01	0.01	0.01	0.01	0.01	0.01	0.00	0.00	0.01
Fe ³⁺	0.75	0.84	0.94	0.96	0.53	0.65	0.55	0.44	0.48	0.52	0.48	0.50	0.46	0.62	0.20	0.26
Mg	2.65	2.31	2.28	2.50	2.77	2.79	2.09	2.40	3.32	3.42	3.07	2.79	3.34	3.27	2.82	3.03
Fe ²⁺	1.00	1.12	1.15	1.02	1.09	0.95	1.82	1.54	0.61	0.49	0.88	1.12	0.64	0.57	1.28	1.11
C sites	5.00	5.00	5.00	5.00	5.00	5.00	5.00	5.00	5.00	5.00	5.00	5.00	5.00	5.00	5.00	5.00
Fe ²⁺	0.20	0.11	0.14	0.17	0.09	0.16	0.01	0.05	0.07	0.06	0.05	0.04	0.05	0.08	0.02	0.04
Mn	0.08	0.06	0.06	0.07	0.03	0.03	0.07	0.04	0.01	0.02	0.03	0.04	0.02	0.02	0.03	0.02
Ca	1.52	1.64	1.57	1.51	1.75	1.60	1.84	1.79	1.82	1.82	1.83	1.83	1.84	1.78	1.80	1.87
Na	0.20	0.19	0.23	0.24	0.13	0.21	0.08	0.12	0.09	0.09	0.09	0.09	0.08	0.12	0.14	0.07
B sites	2.00	2.00	2.00	2.00	2.00	2.00	2.00	2.00	2.00	2.00	2.00	2.00	2.00	2.00	2.00	2.00
Na	0.20	0.27	0.31	0.25	0.40	0.43	0.35	0.44	0.54	0.53	0.58	0.55	0.62	0.53	0.49	0.49
K	0.04	0.06	0.07	0.05	0.09	0.07	0.27	0.27	0.16	0.14	0.14	0.13	0.15	0.13	0.17	0.14
A sites	0.24	0.33	0.38	0.30	0.49	0.50	0.62	0.70	0.70	0.67	0.72	0.68	0.77	0.65	0.66	0.63
OH	1.96	2.63	2.78	1.94	1.94	2.00	2.69	2.60	1.90	1.98	1.94	1.96	1.96	1.97	1.90	1.90
Mg#	0.69	0.65	0.64	0.68	0.70	0.72	0.53	0.60	0.83	0.86	0.77	0.70	0.83	0.87	0.68	0.73
Modif. Name	ferro tsch	ferro tsch	ferro tsch	ferro tsch	tsch	tsch	pts mgbas	pts mgbas	mgbas	mgbas	mgbas	mgbas	mgbas	mgbas	parg	parg

rocks and cognate enclaves. Some amphiboles (e.g. Arsenite microdiorite) display Mg-richer core and Fe-richer rim, while other amphiboles (e.g. Sturzii dacite) display reverse zonation with Mg-richer rim and Fe-richer core.

Pyroxenes are present only in the more basic petrographic types, where they are subordinated in abundance to the amphiboles. They are also found in some mafic magmatic cognate enclaves. In some cognate enclaves pyroxene is the only mineralogical component. Only clinopyroxene occurs in the studied rocks (Table 2). Within the cognate enclaves mostly diopside is present, while augite occurs mainly in the host-rocks. Occasionally, clinoenstatite was found in the pyroxenite enclaves within the Arsenite microdiorite.

Biotite is present in the more acidic petrographical types either as the only mafic mineral (Parva rhyolite) or in association with amphiboles (Ilva rhyodacites and dacites, as well as Valea Vinului quartz biotite andesites). It is also present in the mafic magmatic cognate enclaves within the Valea Vinului Intrusive Unit, where it has a slightly different chemical composition compared with the host-rock biotite. This corresponds to higher Al and Fe, and to lower Mg content.

Plagioclase feldspars are the main components of all the petrographic types; they form both phenocrysts and microlites in the matrix. Anorthite content varies according to the petro-

graphic type: between 20–25 % (oligoclase) in acid rocks, and between 55–76 % (labrador–bytownite) in most microdiorites and basaltic andesites (Table 3). The plagioclases in Chicera and Heniu Magmatic Units (microdiorites, amphibole andesites) are even more basic, with an anorthite content of 70–80 %. Plagioclase feldspars frequently show normal and oscillatory zoning, which is best shown in samples of the Arsenite, Valea Vinului, Cornii and Sturzii Units, indicating modification of crystallization conditions (i.e. magma chamber refilling and/or rapid cooling during the emplacement of the intrusive body).

Potassic feldspars are present in very small amounts (0–4 wt. %), mostly in the cognate enclaves or in the form of microlites in the matrix of the more acidic petrographic types (Valea Vinului). They form totally subordinated phenocrysts in porphyritic microgranodiorites. They are mostly orthoclase. In many cases they are replaced by sericite, kaolinite and calcite.

Garnets are present only in the Pleşii-Mal quartz andesites and Sturzii dacite, as 1–2 wt. % of the rock volume. They form phenocrysts with subhedral or euhedral morphologies, 0.5–2.5 mm in size, and have almandine-rich compositions (over 55 %) (Table 4). Garnets are fresh, without inclusions and reaction zones. Most are found as inclusions in plagioclase.

Table 2: Representative microprobe analyses of pyroxenes of host rocks and enclaves. Abbreviation: **en** — enclave.

Sample Analysis Location	I5 Rock Chicera	I4 rock Arsenite	I4/A2 en Arsenite	I4px0 en Arsenite	I4px0 en Arsenite	I4px1 en Arsenite	I4px2 en Arsenite	I4px4 en Arsenite	I14 en Cornii	I6 en(cor) Runc	I6 en(rim) Runc
SiO ₂	52.13	52.07	51.12	53.65	55.14	52.54	52.83	52.25	50.67	51.84	51.59
Al ₂ O ₃	1.56	1.28	3.18	1.77	1.83	1.85	1.52	2.25	3.84	2.08	2.14
TiO ₂	0.63	0.28	0.56	0.24	0.13	0.20	0.20	0.11	0.72	0.62	0.58
Cr ₂ O ₃	0.10	0.07	0.05	0.52	0.34	0.14	0.10	0.00	0.00	0.00	0.00
FeO*	8.17	9.29	6.30	3.92	11.15	5.27	5.46	6.40	6.70	9.44	9.41
MnO	0.48	0.46	0.24	0.20	0.25	0.13	0.24	0.27	0.24	0.37	0.39
MgO	14.69	14.14	15.62	17.03	30.08	15.51	15.21	15.59	13.70	15.22	14.94
CaO	20.86	21.59	21.87	22.50	0.67	24.18	24.00	22.39	23.69	19.97	20.33
K ₂ O	0.04	0.03	0.03	0.01	0.01	0.00	0.00	0.00	0.02	0.03	0.02
Na ₂ O	0.50	0.25	0.31	0.21	0.02	0.13	0.13	0.30	0.41	0.29	0.27
BaO	0.00	0.03	0.00	0.02	0.00	0.00	0.00	0.00	0.02	0.00	0.00
F	0.11	0.24	0.00	0.03	0.00	0.14	0.20	0.31	0.00	0.00	0.23
Total	99.26	99.72	99.27	100.00	99.60	100.09	99.90	99.90	100.06	99.86	99.91
WO	43.41	44.17	44.90	45.54	1.30	48.39	48.37	45.40	49.19	40.91	41.68
EN	42.53	40.26	44.62	47.95	81.40	43.18	42.66	44.02	39.58	43.39	42.62
FS	14.06	15.57	10.48	6.51	17.30	8.43	8.97	10.58	11.23	15.70	15.70

Table 3: Representative microprobe analyses of feldspars of host rocks and enclaves. Abbreviation: **en** — enclave.

Sample Analysis Location	I15 rock core Sturzii	I15 rock middle Sturzii	I15 rock rim Sturzii	I31 rock Pleşii	I8 rock Heniu	I8/hb1 en Heniu	I8/hb2 en Heniu	I4/A2 en core Arsenite	I4/A2 en middle Arsenite	I4/A2 en rim Arsenite	I4mega en Arsenite	I6 rock Runc
SiO ₂	55.42	57.43	56.25	57.15	50.97	52.04	64.54	55.40	54.46	56.33	65.03	51.66
Al ₂ O ₃	27.78	26.38	27.18	26.40	30.56	29.57	18.18	27.23	28.00	26.62	18.31	29.66
CaO	10.29	8.59	9.59	8.71	13.67	12.81	0.17	9.81	10.77	9.31	0.11	13.08
MnO	0.11	0.00	0.00	0.11	0.04	0.03	0.00	0.00	0.00	0.00	0.00	0.04
FeO*	0.14	0.07	0.07	0.09	0.25	0.24	0.16	0.28	0.29	0.29	0.06	0.63
BaO	0.00	0.05	0.04	0.01	0.00	0.03	0.11	0.00	0.06	0.03	0.10	0.00
Na ₂ O	5.70	6.65	6.07	6.43	3.75	4.26	0.66	5.93	5.14	6.13	0.39	4.00
K ₂ O	0.16	0.15	0.14	0.17	0.07	0.09	15.38	0.38	0.32	0.33	15.99	0.20
Total	99.60	99.33	99.33	99.07	99.34	99.05	99.19	99.03	99.04	99.04	100.00	99.30
Ab	49.59	57.83	52.97	56.60	33.00	37.40	6.00	51.12	45.49	53.32	3.60	35.20
An	49.49	41.29	46.25	42.40	66.50	62.10	0.80	46.71	52.67	44.77	0.00	63.70
Or	0.92	0.88	0.78	1.00	0.50	0.50	93.10	2.17	1.84	1.91	96.40	1.10

Table 4: Representative microprobe analyses of garnets. Abbreviations: **plz** — plagioclase; **hbl** — hornblende.

Sample	Pleșii											
Analysis	in plz rim	middle	core	in plz 1	(from rim to core) 2	3	4	5	6	in hbl rim	middle	core
SiO ₂	37.69	37.90	37.90	37.52	37.79	37.70	37.67	37.52	37.55	37.42	37.63	37.71
TiO ₂	0.19	0.16	0.06	0.23	0.09	0.13	0.21	0.25	0.28	0.29	0.21	0.18
Al ₂ O ₃	20.78	20.82	20.87	20.60	20.85	20.58	20.59	20.55	20.81	20.29	20.5	20.75
Cr ₂ O ₃	0.08	0.00	0.00	0.00	0.00	0.00	0.00	0.08	0.00	0.00	0.00	0.00
MgO	5.81	5.57	5.68	5.60	5.45	5.25	5.05	4.6	5.35	5.35	5.42	5.45
CaO	5.22	5.37	4.51	4.74	5.35	4.66	5.65	4.35	5.11	4.95	4.58	5.13
MnO	3.85	3.45	4.15	4.03	3.59	4.52	3.75	5.22	4.11	3.55	3.99	3.65
FeO	27.35	27.51	27.72	28.14	27.87	28.05	28.03	27.69	27.73	28.36	28.56	28.07
Total	100.97	100.78	100.89	100.86	100.99	100.89	100.95	100.26	100.94	100.20	100.89	100.94
End members												
Uv	0.24	0.00	0.00	0.00	0.00	0.00	0.00	0.24	0.00	0.00	0.00	0.00
Adr	0.53	0.45	0.17	0.63	0.25	0.37	0.59	0.72	0.79	0.80	0.59	0.51
Grs	13.29	13.95	11.91	11.95	14.00	12.08	14.47	11.17	12.86	12.46	11.60	13.17
Alm	56.49	57.53	57.96	58.29	57.97	58.49	58.31	59.09	57.80	59.29	59.34	58.42
Sps	8.06	7.31	8.79	8.46	7.56	9.55	7.90	11.28	8.68	7.53	8.40	7.69
Prp	21.39	20.77	21.17	20.68	20.22	19.51	18.73	17.50	19.87	19.92	20.07	20.21
Sum	100.00	100.00	100.00	100.00	100.00	100.00	100.00	100.00	100.00	100.00	100.00	100.00

clase and rarely in hornblende phenocrysts. Garnets occur either in the core of their host crystals or they can have a peripheral position. The optical and chemical features of the plagioclases hosting garnet crystals are similar to other plagioclases in the rocks.

The presence of the assemblage amphibole-biotite-quartz-plagioclase-K-feldspar-magnetite in lithologies like Sturzii dacite and Valea Vinului andesites recommend that the Al-content in hornblende geobarometer of Johnson & Rutherford (1989) may be applied for pressure estimations. Assuming temperatures close to the range over which this barometer has been calibrated (740–780 °C) pressures of 550–800 MPa have resulted. The same barometer has been tentatively applied for others intrusive units (Pleșii, Cornii, Chicera, Arsente, Heniu, Iliuța) resulting in pressures within the same range, both for host-rocks and cognate enclaves. Slightly higher pressure values have been obtained in the case of cognate enclaves compared with their host-rocks. The highest pressure has been found for the Sturzii dacite. Significant differences are recorded between the pressure values corresponding to the core of the crystals from Sturzii dacite (~780 MPa) and the pressure value corresponding to the rim (~490 MPa). This finding implies that decompression occurred during crystallization of amphiboles. The pressure estimates for host-rocks and cognate enclaves suggest mid-crustal depths of approximately 15–25 km for amphibole crystallization.

Major and trace element geochemistry

Major and trace elements compositions of the host-rocks and cognate enclaves are presented in Table 5. SiO₂ ranges between 39.81 wt. % and 49.87 wt. % in the mafic magmatic cognate enclaves, and from 52.42 wt. % (Colibița andesite) to 75.39 wt. % (Parva rhyolite) in the host-rocks. This variation corresponds to basalts, basaltic andesites, andesite, dacites and rhyolite. Two series of rocks can be seen in the K₂O–SiO₂ dia-

gram (LeMaitre 1989) (Fig. 2). The first series comprises andesites and microdiorites from South Bârgău (Heniu, Oala), the quartz garnet andesites (Pleșii-Mal), Sturzii-Bucnitori dacites and Parva rhyolites and lies in the medium- to low-K domain. The second series contains some of the basaltic andesites, Măguri and Cornii andesites and microdiorites, and Valea Vinului biotite quartz andesites. It trends towards the high-K field. It is worth noting that within the medium-K series amphiboles are the only mafic minerals, while within the high-K series clinopyroxenes, amphiboles and biotites all occur. The cognate enclaves fall mostly in the domain of basalts, with SiO₂ less than 50 wt. %, and K₂O less than 1 wt. %, except those from the Valea Vinului and Arsente which are enriched in K₂O due to high biotite content.

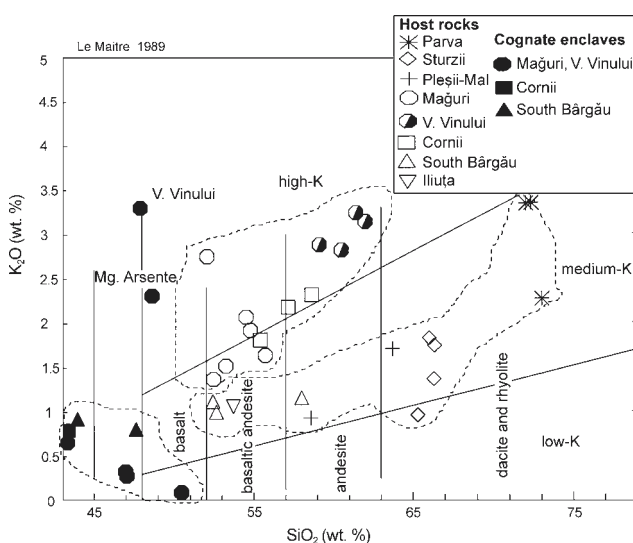


Fig. 2. SiO₂ vs. Na₂O+K₂O diagrams for Rodna-Bârgău igneous rocks showing the separation of two series of rocks.

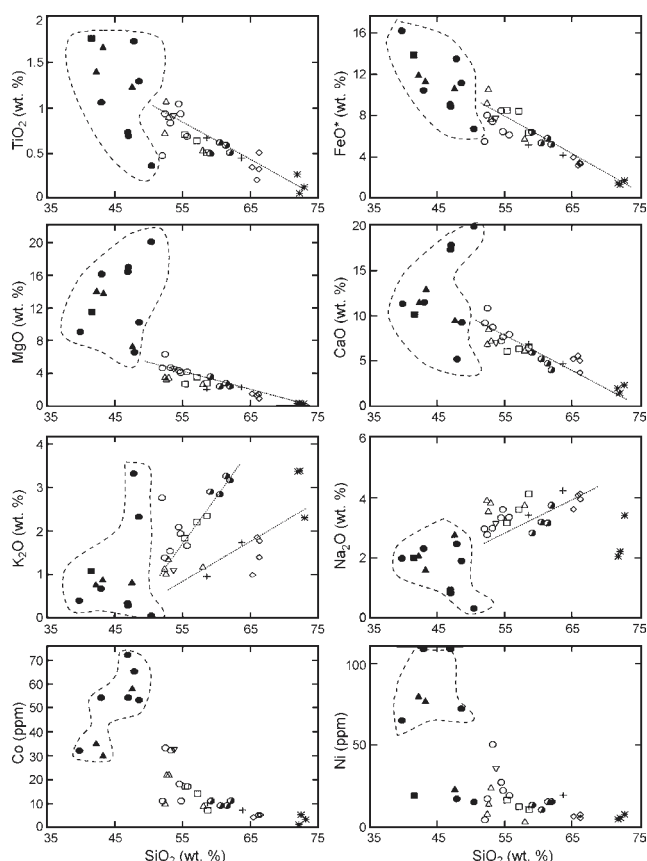


Fig. 3a. Major and trace element for Rodna-Bârgău igneous rocks. Symbols as in Fig. 2.

In the host rocks, variation trends of TiO_2 , FeO^* , MgO , and CaO with SiO_2 content show negative correlations, whereas K_2O and Na_2O increase with increasing SiO_2 (Fig. 3a). The major element variation of the cognate enclaves is more scattered. The compatible trace element contents (Ni, Cr, Co) are higher in the cognate enclaves compared with the host rocks (Table 5). The variation with SiO_2 of these elements is contrasting in cognate enclaves (increasing as SiO_2 increases) and in host-rocks (decreasing as SiO_2 increases). A better correlation was obtained for host-rocks as compared to cognate enclaves. Rb, Nb, Pb, Sr, Zr and Y show a scattered variation with SiO_2 (Fig. 3b). The two series of rocks distinguished according to the K_2O - SiO_2 diagram are also discriminated on the Rb- SiO_2 variation diagram. The variation of Y in cognate enclaves clearly exceeds that of the host-rocks. The Sr and Zr contents in cognate enclaves are slightly lower than in the host-rocks.

The incompatible trace elements and the REE compositions are similar for both host-rocks and cognate enclaves (Table 5). However, the cognate enclaves are less enriched in incompatible trace elements and more heterogeneous than the host-rocks. The REE patterns of rocks (Fig. 4) correspond to those from arcs associated with subduction areas (Wilson 1989) and resemble the neighbouring areas of the Carpathian arc (Downes et al. 1995; Mason et al. 1996). They are LREE enriched, while the HREE pattern is similar to the primitive mantle.

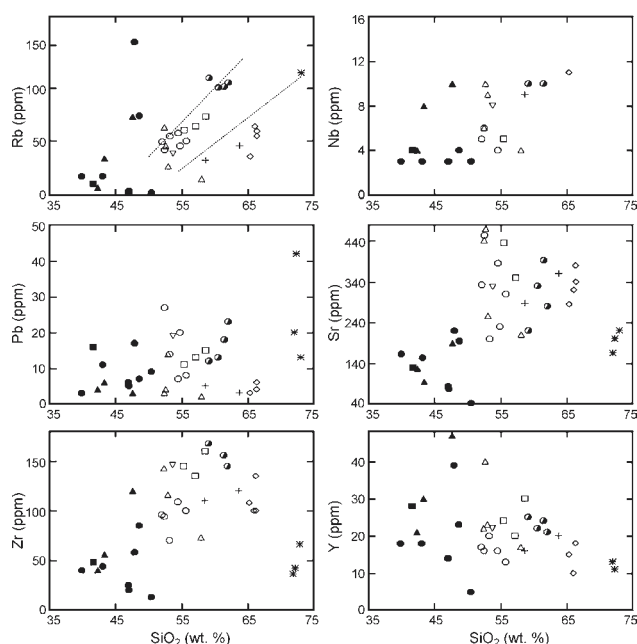


Fig. 3b. Harker variation diagrams for Rodna-Bârgău igneous rocks. Symbols as in Fig. 2.

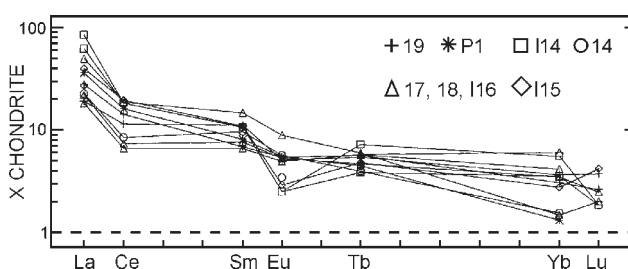


Fig. 4. Chondrite-normalized rare earth elements diagram for representative rocks. Normalized coefficient from Sun & McDonough (1989). Symbols as in Fig. 2 and sample names as in Table 5.

Isotopic composition of the magmatic rocks

Table 6 summarizes the oxygen and strontium isotope analyses performed on host-rocks and cognate enclaves from the main intrusive units. Mineral separates, mostly amphibole and pyroxene, were analysed for O isotope ratio because whole-rock $\delta^{18}\text{O}$ values can often be affected by low-temperature processes such as hydration and weathering, which are characterized by large ^{18}O enrichment effects.

Our samples display $\delta^{18}\text{O}$ values between 3.7 and 6.7 ‰ (SMOW). These values are lower than the expected values for pyroxene and hornblende in typical continental margin arc volcanic rocks (e.g. Hoefs 1997). The variation of $\delta^{18}\text{O}$ values reported for the neighbouring areas (Neogene magmatites from Călimani-Gurghiu-Harghita Mountains (Mason et al. 1996)) and Ukrainian Neogene volcanic arc (Seghedi et al. 2001) is clearly different (5.1 to 8.7 ‰ and 6.1 to 8.3 ‰ respectively) (see also Fig. 7).

Using mineralogical (clinopyroxene vs. amphibole), petrographical (xenolith vs. host-rock) and geochemical (medium-

Table 5: Major and trace element data for Rodna-Bărgău igneous rocks. Major elements are given in percent (%) and trace elements in ppm. Abbreviations: **ba** — basaltic andesite; **pa** — pyroxene andesite; **aa** — amphibole andesite; **qba** — quartz biotite andesite; **qga** — quartz garnet andesite; **md** — microdiorites; **d** — dacite; **r** — rhyolite; **nd** — not determined. Total iron is expressed as FeO.

Sample Location Rock type	P1 Parva r	P2 Parva r	P3 Parva r	I15 Sturzii d	P21 Sturzii d	P22 Bucnitiori d	P23 Bucnitiori d	I10* V.Vin. qba	I11 V.Vin. qba	P13 V.Vin. qba	P14 V.Vin. a	P4 Plesii qga	I9 Mal qga	I14* Cornii aa	P82 Cornii aa	P108 Cornii aa	I4 Arsente md	P62 Arsente md	I5* Chicera md	P71 Chicera md
SiO ₂	75.39	74.17	74.52	65.30	67.22	66.53	67.27	60.33	61.42	63.95	63.22	64.92	58.60	58.23	59.36	58.17	54.50	55.93	53.12	54.23
TiO ₂	0.17	0.05	0.12	0.34	0.33	0.20	0.52	0.49	0.58	0.54	0.64	0.45	0.66	0.64	0.51	0.61	1.04	0.92	0.47	0.84
Al ₂ O ₃	14.53	15.18	15.26	17.30	16.16	16.14	16.98	15.01	16.69	16.07	16.14	16.98	18.97	18.4	17.74	16.53	17.77	18.14	19.96	17.69
FeO*	1.41	1.25	1.65	3.87	3.40	3.13	3.33	6.83	5.70	6.45	5.49	4.15	5.07	8.43	6.31	7.23	8.24	6.23	5.43	7.54
MnO	0.07	0.06	0.04	0.11	0.10	0.09	0.09	0.24	0.13	0.11	0.13	0.09	0.16	0.15	0.14	0.17	0.24	0.14	0.05	0.14
MgO	0.20	0.30	0.20	1.44	1.38	1.26	0.86	3.68	2.73	2.43	2.45	2.27	1.98	2.62	2.7	3.52	4.28	4.14	4.62	4.78
CaO	1.49	1.41	1.98	5.17	5.06	5.58	3.87	5.88	4.68	0.07	5.41	4.71	6.83	6.01	6.47	6.41	7.18	7.25	9.45	8.84
Na ₂ O	2.10	2.25	3.23	3.59	3.89	4.11	4.05	2.8	3.13	3.83	3.31	4.05	3.4	3.14	4.15	3.64	3.32	3.58	3.05	3.05
K ₂ O	3.50	3.47	2.32	0.96	1.39	1.86	1.81	2.88	3.24	3.24	2.95	1.15	0.93	1.81	2.35	2.66	2.07	1.89	2.75	1.56
P ₂ O ₅	0.05	0.04	0.16	0.26	0.09	0.08	0.10	0.23	0.3	0.60	0.27	0.09	0.02	0.16	0.20	0.21	0.23	0.18	0.06	0.18
H ₂ O	2.36	2.17	1.28	0.95	1.14	1.41	1.30	0.89	1.11	1.97	0.66	1.68	2.9	0.18	0.90	1.00	1.63	1.77	1.12	1.41
Total	100.27	100.35	100.76	99.29	100.16	100.39	100.18	99.26	99.71	99.26	100.67	100.54	99.52	99.77	100.83	100.15	100.50	100.17	100.08	100.28
Rb	189	nd	128	39	61	71	67	120	111	118	115	51	35	66	81	71	63	51	54	62
Sr	173	207	225	287	386	325	351	420	393	288	345	368	287	435	482	358	386	235	333	207
Y	14	11	nd	15	nd	10	19	25	24	22	23	20	16	24	30	20	16	nd	17	21
Zr	39	44	67	111	137	101	103	168	156	150	188	123	110	145	162	138	109	nd	96	73
Nb	nd	nd	nd	11	nd	nd	nd	10	10	nd	nd	nd	9	5	nd	nd	4	nd	5	nd
Pb	21	42	13	3	4	nd	6	12	18	24	14	3	5	11	15	13	36	20	58	16
Ga	8	nd	11	15	15	nd	12	29	17	19	21	18	18	16	16	16	21	25	6	15
Zn	nd	52	47	45	42	nd	45	78	120	125	73	92	90	71	114	71	41	nd	59	59
Ni	4	5	7	6	7	nd	5	13	15	15	10	19	12	16	10	12	27	22	4	51
Co	1	5	3	4	5	5	5	11	9	11	9	7	10	17	7	14	18	11	11	33
Ba	325	601	378	220	376	403	516	1023	1010	746	993	307	300	844	772	821	426	327	95	246
Cr	5	6	10	11	10	10	19	43	40	84	84	11	46	36	32	21	38	92	253	236
V	14	23	18	45	66	nd	36	122	112	108	136	72	75	153	122	132	179	107	150	226
Sc	nd	nd	nd	8	10	6	6	13	15	12	15	10	12	23	12	28	17	nd	9	nd
Cu	65	13	20	22	10	nd	8	36	20	39	31	38	23	34	38	35	76	53	46	65
Sn	nd	nd	nd	nd	2.03	nd	2.06	1.14	2.00	2.06	2.09	nd	2.50	2.00	2.02	nd	nd	nd	nd	nd
La	23.77	24.89	nd	25.00	30.49	17.25	33.03	36.00	31.00	43.27	62.70	17.91	12.00	39.00	53.65	32.56	14.60	nd	3.80	nd
Ce	26.70	nd	nd	31.00	nd	31.45	nd	nd	nd	nd	nd	23.03	18.00	29.00	29.36	nd	13.30	nd	4.80	nd
Sm	3.35	nd	nd	4.33	nd	4.36	nd	nd	nd	nd	nd	2.76	4.40	4.20	4.25	nd	3.8	nd	1.30	nd
Eu	0.85	nd	nd	0.43	nd	0.44	nd	nd	nd	nd	nd	0.82	0.75	0.37	0.37	nd	0.84	nd	0.51	nd
Tb	0.45	0.93	nd	0.46	nd	0.16	nd	nd	nd	nd	nd	0.55	0.52	0.69	0.37	nd	0.38	nd	0.43	nd
Yb	0.61	nd	nd	1.20	1.63	0.88	1.45	2.40	nd	2.47	2.61	1.35	1.58	2.38	1.55	2.54	0.67	nd	0.79	nd
Lu	nd	nd	nd	0.27	nd	0.27	nd	nd	nd	nd	nd	0.17	0.24	0.12	0.12	nd	nd	nd	nd	nd
Cs	9.42	nd	nd	nd	nd	0.51	nd	nd	nd	nd	nd	0.31	nd	2.80	nd	nd	1.20	nd	nd	nd
Th	10.16	nd	nd	4.40	nd	4.46	nd	11.00	11.10	11.64	11.49	1.64	1.00	4.00	4.05	nd	4.30	nd	1.60	nd
Hf	1.99	nd	nd	2.60	nd	nd	nd	nd	nd	nd	nd	1.54	1.50	2.50	nd	nd	nd	nd	nd	nd
Ta	2.41	nd	nd	1.20	nd	nd	nd	nd	nd	nd	nd	1.02	0.50	1.40	nd	nd	nd	nd	nd	nd

K vs. high-K series) criteria, several groups of $\delta^{18}\text{O}$ values have been delimited. Descriptive statistics of the $\delta^{18}\text{O}$ values is presented in Table 7. For comparison, the variation of the $\delta^{18}\text{O}$ values in mantle clinopyroxenes (amphiboles present) is also shown (data from Matthey et al. 1994). To test for significant differences between means, one-way analysis of variance test (ANOVA) has been performed giving $p=0.0026$ (differences are significant at $p<0.05$). The pyroxenes from cognate enclaves show the closest values to the mantle. Comparable values were found in Iliuța basaltic andesite. The lowest values are shown by the Măguri andesites (high-K series). The highest $\delta^{18}\text{O}$ values were found in the Cornii (6.6‰) and Colibița andesites (6.7‰). The most scattered values are shown by amphiboles from the cognate enclaves. In some of the analysed enclaves (I4px1, I4px2, I4px4, I8/hb2) isotopic

disequilibria between amphiboles and coexisting pyroxenes can be observed.

The $\delta^{18}\text{O}$ value for garnet from the Pleșii quartz garnet andesite (4.3‰) lies within the range of the δ -values exhibited by the amphiboles from the medium-K series. Much higher $\delta^{18}\text{O}$ value (7.3‰) was obtained for the metamorphic garnet (alm 61 %; and 23 %; sps 4 %; prp 12 %) from the staurolite garnet micaschists within the Rebra series. The $\delta^{18}\text{O}$ value of the Pleșii garnet is lower than the values for garnet reported in the literature (Harangi et al. 2001 and literature there in). For the Carpatho-Pannonian region the $\delta^{18}\text{O}$ values of the igneous almandine garnet range from 6.1 to 10.5‰ (Mason et al. 1996; Harangi et al. 2001).

Age correction of the measured $^{87}\text{Sr}/^{86}\text{Sr}$ ratio values (using data from Pécskay et al. 1995) has been performed in order to

Table 5: Continuing.

Sample Location Rock type	P95 Chicera md	I6 Runc pa	P11 Heniu aa	I8' Heniu aa	I7' Oala aa	I16 Colibita aa	I18' Iliuța ba	Cognate enclave	I10/en V.Vin.	I14/en Cornii	I4/A2 Arsente	I4/A3 Arsente	I4 px0 Arsente	I4 px 1 Arsente	I4 px 4 Arsente	I5/en Chicera	I8/hb2 Heniu	I8/hb1 Heniu	I16/en Colibita
SiO ₂	56.93	52.46	52.83	53.08	58.96	52.42	53.78	SiO ₂	47.91	41.68	48.62	42.52	49.87	46.97	47.05	39.81	43.31	42.33	47.62
TiO ₂	0.65	0.93	1.07	1.12	0.67	0.72	0.95	TiO ₂	1.73	1.86	1.29	1.17	0.35	0.73	0.69	2.00	1.67	1.40	1.23
Al ₂ O ₃	17.51	17.02	18.78	18.15	17.82	18.94	18.76	Al ₂ O ₃	16.65	13.98	14.05	13.25	2.42	7.00	6.35	16.66	12.25	13.70	17.75
FeO*	6.27	7.98	10.60	8.17	5.86	9.21	7.69	FeO*	13.47	14.15	11.13	10.43	6.63	9.06	8.85	16.20	11.34	11.95	10.66
MnO	0.10	0.17	0.17	0.26	0.15	0.18	0.17	MnO	0.29	0.31	0.21	0.18	0.12	0.16	0.15	0.21	0.19	0.14	0.17
MgO	4.15	6.31	3.27	3.49	2.69	3.56	4.93	MgO	6.55	11.50	10.23	14.89	19.56	16.42	16.98	9.09	13.86	14.17	7.34
CaO	8.15	10.81	8.57	7.69	6.17	6.88	6.90	CaO	5.19	10.16	9.23	11.53	19.83	17.31	17.81	11.34	12.98	11.52	9.51
Na ₂ O	3.42	2.76	3.56	3.81	3.88	3.91	3.89	Na ₂ O	2.45	1.99	1.88	2.33	0.31	0.93	0.82	1.98	1.60	2.08	2.77
K ₂ O	1.69	1.37	1.00	1.34	1.18	1.12	1.06	K ₂ O	3.3	1.17	2.31	0.68	0.04	0.33	0.28	0.39	0.87	0.76	0.81
P ₂ O ₅	0.14	0.12	0.13	0.14	0.19	0.2	0.17	P ₂ O ₅	0.12	0.19	0.06	0.1	0	0.09	0.02	0.11	0.05	0	0.06
H ₂ O	1.67	0.96	0.75	2.10	2.11	2.06	1.07	H ₂ O	2.56	2.25	1.00	2.26	0.89	1.00	1.00	1.88	1.77	2.11	1.94
Total	100.68	100.89	100.73	99.35	99.68	99.20	99.37	Total	100.22	99.24	99.34	73.39	100.02	100.00	100.00	99.67	99.89	100.16	99.89
Rb	57	46	50	29	16	69	42	Rb	157	11	81	19	2	2	4	19	37	7	80
Sr	319	454	472	256	210	442	327	Sr	220	129	195	154	41	83	77	163	94	127	190
Y	14	16	40	23	17	22	22	Y	39	28	23	18	5	14	14	18	30	21	47
Zr	102	94	181	116	73	143	146	Zr	58	48	85	44	13	25	20	40	56	40	120
Nb	nd	6	10	9	4	6	8	Nb	16	4	4	3	3	3	3	8	4	4	10
Pb	8	27	4	14	2	3	5	Pb	17	16	7	11	9	6	5	14	6	4	3
Ga	21	27	19	16	18	17	19	Ga	32	26	14	14	20	11	10	13	13	13	22
Zn	74	nd	77	nd	nd	57	nd	Zn	nd	nd	73	217	nd	42	37	nd	nd	nd	nd
Ni	20	17	14	24	2.5	8	35	Ni	17	19	72	82	15	109	109	65	77	80	23
Co	18	33	22	22	9	10	32	Co	65	21	53	54	23	72	54	32	30	35	58
Ba	432	460	231	310	550	270	240	Ba	1000	0	584	210	19	77	70	40	nd	0	115
Cr	70	35	48	320	44	19	130	Cr	6	70	111	38	60	378	370	nd	80	58	38
V	237	340	191	320	120	160	240	V	300	28	411	334	300	273	267	320	450	330	440
Sc	26	34	28	25	11.7	15	28	Sc	90	15	nd	nd	22	nd	nd	0	90	280	80
Cu	62	210	32	35	32	43	110	Cu	210	50	nd	nd	43	nd	nd	63	65	62	310
Sn	nd	nd	21	2	2.5	nd	3	Sn	5.5	3	nd	nd	0	nd	nd	0	3	3	2
La	nd	nd	11.41	11.43	31.31	13.85	30.00	La	<30	nd	<30	<30	<30	<30	<30	30	nd	nd	nd
Ce	nd	nd	10.40	10.42	29.71	11.68	nd	Ce	nd	nd	37	39	nd	37	30	nd	nd	nd	nd
Sm	nd	nd	2.61	2.65	5.82	3.00	nd	Sm	nd	nd	nd	nd	nd	nd	nd	nd	nd	nd	nd
Eu	nd	nd	0.73	0.73	1.32	0.78	nd	Eu	nd	nd	nd	nd	nd	nd	nd	nd	nd	nd	nd
Tb	nd	nd	0.55	0.55	0.57	0.45	nd	Tb	nd	nd	nd	nd	nd	nd	nd	nd	nd	nd	nd
Yb	nd	3.00	2.61	1.85	0.64	1.55	3.00	Yb	7	3	nd	nd	nd	nd	nd	nd	nd	nd	5
Lu	nd	nd	nd	nd	0.13	0.16	nd	Lu	nd	nd	nd	nd	nd	nd	nd	nd	nd	nd	nd
Cs	nd	nd	1.91	nd	2	nd	nd	Cs	nd	nd	nd	nd	nd	nd	nd	nd	nd	nd	nd
Th	nd	4.30	2.71	2.73	12.21	4.00	10.00	Th	nd	nd	3	<2	nd	<2	<2	nd	nd	nd	nd
Hf	nd	nd	2.01	nd	nd	nd	nd	Hf	nd	nd	nd	nd	nd	nd	nd	nd	nd	nd	nd
Ta	nd	nd	0.53	nd	nd	nd	nd	Ta	nd	nd	nd	nd	nd	nd	nd	nd	nd	nd	nd

obtain the initial $^{87}\text{Sr}/^{86}\text{Sr}$ ratios (Table 6). The differences between corrected and uncorrected values are negligible. The initial $^{87}\text{Sr}/^{86}\text{Sr}$ ratios have been used in all diagrams. The total range of $^{87}\text{Sr}/^{86}\text{Sr}$ ratios is from 0.70588 to 0.70950. The lowest value is from the Iliuța basaltic andesite from the medium-K series. Variation curves of the host-rocks from medium-K and high-K series plot as distinctive straight lines on the $^{87}\text{Sr}/^{86}\text{Sr}$ vs. $1/\text{Sr}$ diagram (Fig. 5), suggesting two-component mixing. The increase of the $^{87}\text{Sr}/^{86}\text{Sr}$ ratios matches the increase of the Sr content in the high-K series. For the medium-K series there is a slightly negative correlation between the two parameters. The cognate enclaves display $^{87}\text{Sr}/^{86}\text{Sr}$ ratios from 0.70620 to 0.70902. On the $^{87}\text{Sr}/^{86}\text{Sr}$ vs. $1/\text{Sr}$ diagram, the pyroxenites and the hornblendites define distinct fields. There is a larger variation of Sr content within the cognate enclaves than in the host rock. The similar $^{87}\text{Sr}/^{86}\text{Sr}$ signature of the cognate enclaves as compared with their host rocks is consistent with their co-magmatic origin. In some cases higher values were found in cognate enclaves relative to their host rock. This could be explained by their relatively low Sr con-

tent (41 to 195 ppm) that made them more susceptible to ^{87}Sr contamination.

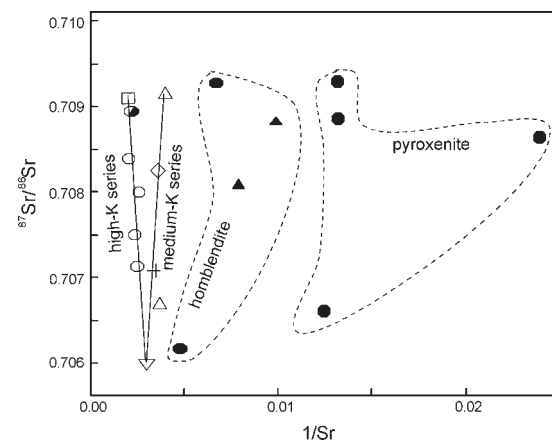


Fig. 5. $^{87}\text{Sr}/^{86}\text{Sr}$ vs. $1/\text{Sr}$ for host-rocks and cognate enclaves in the Rodna-Bârgău Mountains.

Table 6: Sr-O isotope analyses for representative host-rocks and cognate enclaves from the Rodna-Bârgău Mountains. Sr isotope data are expressed as measured and age (10.6–8.6 Ma) corrected $^{87}\text{Sr}/^{86}\text{Sr}$ ratios.

Series	Sample	Location	Rock type	$^{87}\text{Sr}/^{86}\text{Sr}$	$^{87}\text{Sr}/^{86}\text{Sr}_i$	$\delta^{18}\text{O}_{\text{cpx}}$	$\delta^{18}\text{O}_{\text{hbl}}$	$\delta^{18}\text{O}_{\text{grt}}$
medium-K	I15	Sturzii	dacite	0.70818	0.70812		4.3	
	I9	Mal	qtz grt andesite	0.70704	0.70699			
	I31	Pleşii	qtz grt andesite				4.8	4.3
	I7	Oala	amph andesite	0.70671	0.70668		5.2	
	I8	Heniu	amph andesite	0.70929	0.70925		4.8	
	I8/hb1	Heniu	hornblende	0.70798	0.70796		5.1	
	I8/hb2	Heniu	hornblende	0.70902	0.70887		4.2	
	I18	Iliuța	basaltic andesite	0.70593	0.70588		5.4	
high-K	I10	V.Vinului	qtz bi andesite	0.7090	0.70889			
	I11	V.Vinului	qtz bi andesite	0.70749	0.70738			
	I4	Arsente	microdiorite	0.70797	0.70791		3.9	
	I4/A2	Arsente	hornblende	0.70620	0.70605		3.8	
	I4mega	Arsente	hornblende	0.70954	0.70950		4.6	
	I4px0	Arsente	pyroxenite	0.70862	0.70860	5.7		
	I4px1	Arsente	pyroxenite	0.70633	0.70632	5.2	4.2	
	I4px2	Arsente	pyroxenite	0.70879	0.70877	4.6	5.2	
	I4px4	Arsente	pyroxenite	0.70941	0.70939	4.6	4.0	
	I5	Chicera	microdiorite	0.70706	0.70700	4.6	3.7	
	I5en	Chicera	hornblende				5.4	
	I14	Cornii	amph andesite	0.7090	0.70891		6.6	
	I14en	Cornii	hornblende			5.7	5.6	
	I6	Runc	px andesite	0.70794	0.70790	5.3		
	I16	Colibița	amph andesite	0.70845	0.70839		6.7	
	I16en	Colibița	hornblende				5.2	
Rebra	5/96	Rodna	micaschist					7.3

Table 7: Summary of the distribution of the $\delta^{18}\text{O}$ values.

	Mantle	Cognate enclaves		Medium-K series	High-K series		Cornii/Colibița
	cpx	cpx	amph	amph	cpx	amph	amph
Mean	5.52	5.30	4.53	4.92	4.95	3.80	6.65
Min.	5.25	4.6	3.8	4.3	4.6	3.7	6.6
Max.	5.75	5.7	5.6	5.4	5.3	3.9	6.7
Std. dev.	0.16	0.52	0.76	0.42	0.49	0.14	–

Discussion

The results of the geochemical study based on the major, minor, rare earth elements, O and Sr isotopes can be used to form a framework for discussion of the petrogenetic processes that influenced the magma evolution in the region.

Processes related to magma differentiation

Differentiation by fractional crystallization is suggested by the existence of a complete series of rocks containing all the petrographic types, from basalts to rhyolites. The presence of a great variety of mineral species: plagioclases, amphiboles, pyroxenes, quartz, biotite, garnets, iron oxides etc. corresponds to a succession of fractional crystallization. The presence of obvious trends of linear correlation of the major elements with differentiation indices (SiO_2) also pleads for magma differentiation (Fig. 3a). Another argument for fractional crystallization is offered by the REE pattern. The negative anomaly of Eu found in all lithologies indicates the importance of plagioclase fractionation. The negative Eu anomaly could also be generated by partial melting with a plagioclase-rich residue. Scattered variations of minor elements with SiO_2 , indicate diverse conditions of differentiation for

different magmatic units. Consequently, each intrusive unit may have encountered specific differentiation processes and possibly did not evolve from a single source.

Similarities in mineralogy of the main mineral species, in P-T conditions of amphibole crystallization, in incompatible trace element patterns, and in strontium and oxygen isotope composition between cognate enclaves and their host rocks, clearly indicate that cognate enclaves formed from the same magmatic source. They could be products of magma mixing processes resulting from repeated feeding of magma chambers with parental mafic melts. This could also explain why cognate enclaves predominantly occur within larger intrusive units with intermediate composition (Heniu, Măguri, Cornii, and Valea Vinului). The maintenance of an intermediate composition during crystallization and crustal rock assimilation involves new inputs of mafic magma. Oscillatory zoning and corrosion shown by plagioclase phenocrysts from Arsente, Valea Vinului and Cornii intrusions might also indicate refill of the magmatic chamber with less evolved melts. However, an alternative possible explanation is that the cognate enclaves represent broken fragments of cumulate layers formed on the floor of the intermediate magma chambers.

Evidence for crustal assimilation

In subduction-related magmatism possible contamination mechanisms are: source contamination related to the descending slab and its sediments, and/or crustal contamination within crustal magma chamber achieved by assimilation-fractional crystallization processes (AFC). The existing geotectonic models in the Carpatho-Pannonian region (e.g. Rădulescu & Săndulescu 1976; Csontos 1995) consider that during the subduction process oceanic crust, thinned continental crust, as well as related sediments (present-time External Carpathian Flysch strata) were consumed.

High $^{87}\text{Sr}/^{86}\text{Sr}$ ratios are usually interpreted in terms of crustal assimilation. As the increase of the $^{87}\text{Sr}/^{86}\text{Sr}$ ratios is also linked to the enrichment of lithophile trace elements as compared to primitive mantle and MORB, crustal assimilation process is to be considered in the petrogenesis of the Rodna-Bârgău magmatites. Crustal assimilation is also proved by the presence of crustal enclaves (metamorphic and sedimentary rocks).

The Th/Nb vs. SiO_2 diagram (Fig. 6) clearly shows discrimination of the two series of rocks. The high-K series is characterized by higher Th/Nb ratio suggesting a more important contribution of the upper crust and/or sediments in their generation, whereas the medium-K series display lower Th/Nb ratios is, therefore, less affected by contamination with such components.

For the medium-K series the most probably contaminant is the lower crust. Its involvement is supported by the presence of garnet-bearing andesites. Petrogenesis of primary garnet-bearing igneous rocks requires special composition and P-T conditions of the magma, as well as special tectonic setting for facilitating rapid ascent of the magma to the surface because of the limited stability field of the garnet. It is explained by partial melting of the lower crust due to the uprising of mantle-derived magmas, producing small volumes of acid rocks with a high content of Al_2O_3 (e.g. Harangi et al. 2001). The assemblage garnet + plagioclase + amphibole + quartz is stable at pressures higher than 800 MPa and temperatures of 800–850 °C in a dacite melt with 5 % H_2O (Day et al. 1992). Such highly hydrated dacite magma can be generated from a basaltic precursor with 2–3 % water (Green 1992). For the garnet bearing andesites (Pleșii-Mal) and dacites (Sturzii) high internal pressure of the magma due to a high H_2O -rich fluid content, and the appearance of a decompression regime could facilitate relatively rapid ascent of magma and preservation of garnets. The occurrence of the Rodna-Bârgău garnet-bearing

rocks close to the Someș Fault and the lack of cognate enclaves, which would indicate the existence of intermediate chambers, are other arguments for a rapid ascent of magma. A hydrous mantle source, which is another essential requirement for the formation of primary garnet-bearing rocks, is consistent with the elevated Ba/La ratio of the rocks from the medium-K series and also with the exclusive occurrence of hydrous mafic minerals within this series. Exploded fluid inclusions, surrounded by other small fluid inclusions, found within quartz grains from Bucnitori dacite, clearly suggest that decompression took place (Papp et al. 2003) facilitating rapid ascent of magma and preservation of garnets. Pressure decreasing, inferred from the chemical composition of amphiboles in Sturzii dacite, also suggests a decompression regime.

Significance of the low oxygen isotope ratios

Different processes could induce depletion in ^{18}O of the magmatic rocks. Typically, low- ^{18}O rocks are interpreted in terms of hydrothermal alteration in the upper crust by interaction with cold meteoric water or seawater. Low temperature (between 200 and 400 °C) hydrothermal systems with short lifetimes ($<10^6$ years) produce large isotopic effects and important isotopic disequilibrium between rock-forming minerals. Other mineralogical and petrographic effects typically occur (Taylor 1974): partial or total alteration of primary mafic minerals, micrographic intergrowths of alkali feldspar and quartz, miarolitic cavities and veins filled with quartz, alkali feldspar, chlorite, etc. Conversely, sub-solidus hydrothermal exchange at very high temperatures (400–800 °C) is compatible with the general absence of hydrous alteration products in the mineral assemblages, with the presence of clinopyroxenes, and with a relatively uniform oxygen isotope composition in all lithologies (Hoefs 1997 and literature therein). In certain cases, low- $\delta^{18}\text{O}$ magmas may be formed by remelting of hydrothermally altered country rocks or by large-scale assimilation of such material.

Hydrothermal alteration products are poorly developed or absent in most of the intrusive bodies under study. δD values measured on whole-rocks (andesites, microdiorites, rhyolites) or amphiboles vary from -55‰ to -75‰ (Papp 1999) and are “normal” values for igneous rocks. Because of the high diffusion rate of hydrogen in rocks, late low-temperature interaction with crustal fluids would have produced important shifts towards low δD values. All these observations, as well as the existence of a correlation between oxygen and strontium isotopic ratios, lead us to discuss the low measured $\delta^{18}\text{O}$ values in terms of primary isotopic characteristics of the parental magmas. However, sub-solidus exchange with meteoric underground water has to be taken into consideration as a complementary process during the cooling history of the rocks, also leading to depletion in ^{18}O .

On the $^{87}\text{Sr}/^{86}\text{Sr}$ vs. $\delta^{18}\text{O}$ diagram (Fig. 7), the *medium-K series* defines a significant negative correlation (correlation coefficient, $r = -0.72$). The trend starts from basaltic andesites (Iliuța) to andesites (Oala), quartz andesites (Pleșii-Mal) and dacites (Sturzii). The decrease of the $\delta^{18}\text{O}$ values as $^{87}\text{Sr}/^{86}\text{Sr}$ ratios and SiO_2 increase is interpreted as a progressive contamination of a mantle-derived magma with a contaminant depleted in

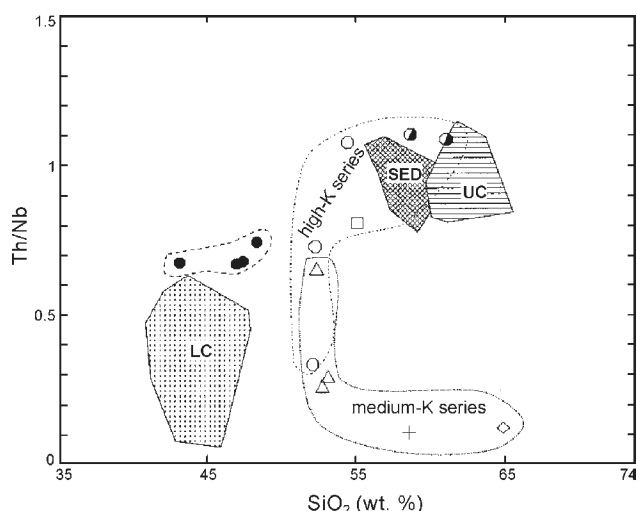


Fig. 6. Th/Nb vs. SiO_2 diagram for Rodna-Bârgău magmatites. Flysch sediments (SED) and upper crust (UC) from Mason et al. (1996), lower crust (LC) from Kempton et al. (1997). Different fields for cognate enclaves, medium-K and high-K series are shown. Symbols as in Fig. 2.

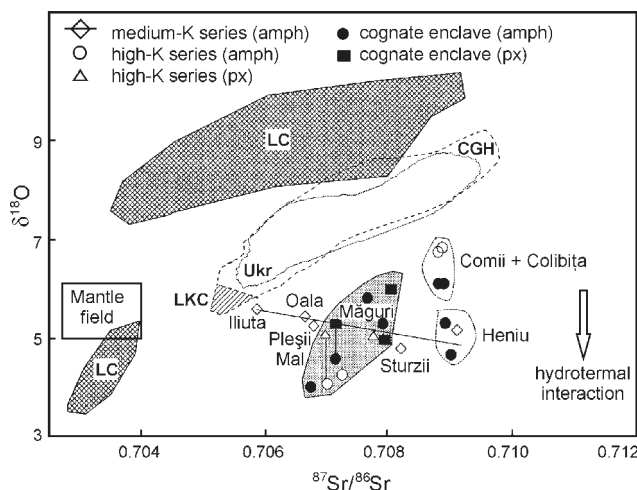


Fig. 7. $\delta^{18}\text{O}$ (mineral separate) vs. $^{87}\text{Sr}/^{86}\text{Sr}$ (whole-rock) diagram for Rodna-Bărgău igneous rocks. Bulk rock fields of Pannonian Basin lower crust (LC) (Kempton et al. 1997) and for East Carpathian arc including Călimani-Gurghiu-Harghita segment (CGH) (Mason et al. 1996) and Ukrainian Carpathians (Ukr) (Seghedi et al. 2001) are also shown for comparison. The Călimani low-K group (LKC) is also highlighted. See text for discussions. Mineral phases from the same rock are indicated by tie lines.

$\delta^{18}\text{O}$ and enriched in $^{87}\text{Sr}/^{86}\text{Sr}$ (i.e. hydrothermally altered crustal rocks). As shown in the previous paragraph lower crust could be taken into consideration as the crustal component. A lower crust characterized by low $\delta^{18}\text{O}$ values ($<4.3\text{‰}$) and medium to high $^{87}\text{Sr}/^{86}\text{Sr}$ ratios (>0.710) has to be assumed in order to explain the isotopic characteristic of these rocks. Kempton et al. (1997) reported similar low $\delta^{18}\text{O}$ values for the lower crust in the Carpatho-Pannonian area, although they correlate with much lower $^{87}\text{Sr}/^{86}\text{Sr}$ ratios (see Fig. 7).

Iliuța basaltic andesite is the least contaminated rock, showing $\delta^{18}\text{O}$ values and $^{87}\text{Sr}/^{86}\text{Sr}$ ratios close to a mantle source. Taking into account its volcanic-like texture and the small volume of the intrusion, we can assume that the magma solidified rapidly near the surface, without important interaction with meteoric water to affect the initial $\delta^{18}\text{O}$ value.

The petrogenesis of primary garnet-bearing rocks (Pleșii-Mal and Sturzii) imply a rapid ascent of magmas, without significant contamination within the middle/upper crust. Garnet is a highly refractory mineral to oxygen isotope exchange. In the Pleșii andesite the garnet appears to be in isotopic equilibrium with the coexisting amphibole (4.8‰). Equilibrium oxygen fractionation between garnet and amphibole is less than 0.4 in the temperature range of $850\text{--}1000\text{ °C}$ (Zheng 1993a,b). Moreover, the garnets of the Pleșii andesite display a significantly different $\delta^{18}\text{O}$ value compared with the garnets of the Rebra series (7.3‰) and therefore a xenocrystic metamorphic origin for the garnets from the quartz andesite could be ruled out suggesting a primary magmatic origin. Taking all these facts into consideration, the garnets of the Pleșii andesite could be indicative for the oxygen isotope composition of the magma from which it crystallized (i.e. 4.3‰).

In spite of its more basic composition relative to the Pleșii quartz andesite and Sturzii dacite, Heniu amphibole andesite

exhibits higher $^{87}\text{Sr}/^{86}\text{Sr}$ ratios and higher $\delta^{18}\text{O}$ value. A process of assimilation and equilibrium crystallization (AEC) (Huppert & Sparks 1985) could be a possible explanation for the increasing $^{87}\text{Sr}/^{86}\text{Sr}$. Hotter and voluminous mafic magmas are able to assimilate more crustal material than cooler less voluminous acid ones. The preservation of an intermediate composition during assimilation and crystallization implies new inputs of mafic magma, which are supported by the presence of cognate enclaves (Heniu is by far the largest intrusive unit).

Within the *high-K series* a correlation between the $\delta^{18}\text{O}$ values, $^{87}\text{Sr}/^{86}\text{Sr}$ ratios and SiO_2 content cannot be identified (Fig. 7). For the Măguri andesites the distribution is scattered. In addition, oxygen isotope disequilibrium between coexisting pyroxenes and amphiboles, both in host-rocks and cognate enclaves have been observed, as well as additional mineralogical and petrographical alteration effects (some alteration of primary mafic minerals, miarolitic cavities and veins filled with quartz and calcite). These features are characteristics of hydrothermal systems with a short lifetime. Therefore, for the Măguri intrusions the most probable explanation for the depletion in ^{18}O is the interaction between intrusive bodies and heated meteoric water. However, the isotopic heterogeneities observed within the Măguri andesites might be due to an inhomogeneous source. This could be an incompletely homogenized MASH zone (mixing, assimilation, storage and homogenization; Hildreth & Moorbath 1988), which operated at the lower-crustal depths. The presence of MASH zones was previously suggested for the Călimani-Gurghiu-Harghita segment (Mason et al. 1996).

Cornii and Colibița andesites, from the *high-K series*, are characterized by the highest $\delta^{18}\text{O}$ (6.7‰) and $^{87}\text{Sr}/^{86}\text{Sr}$ ratio (0.709), which imply extensive crustal assimilation. These rocks are well crystallized, and have high K and Sr contents. They form large intrusions. All these features can be explained by stagnation of magma in large chambers, situated in the mid-crustal depth, where AFC processes took place. Distinctive equilibrium mantle-like $\delta^{18}\text{O}$ values of the pyroxene and amphibole from the cognate enclaves within Cornii andesite indicate an origin from a mantle-derived uncontaminated source. The higher $\delta^{18}\text{O}$ values of the host rocks are not consistent with assimilation of a highly altered crust.

Conclusions

The geotectonic evolution and the magmatic processes in the Rodna-Bărgău Mountains are an intrinsic part of the general evolution of the Carpatho-Pannonian region during Tertiary times. The East Carpathian magmatic arc is closely related to the subduction processes located at the southwestern border of the Eurasian plate.

The results of the mineralogical and geochemical study (major and trace elements, oxygen and strontium isotopes) allowed us to evaluate the petrogenetic processes which influenced magmatic evolution. Each intrusive unit encountered specific differentiation processes by fractional crystallization, crustal assimilation and magma mixing. Two different series of rocks have been separated: one medium-K and another high-K.

The rocks of the *medium-K series* are the oldest, being emplaced at about 10.6 Ma. Mantle-derived magma, contaminated with lower-crustal material is considered to be the source of these rocks. The magmas had a rapid ascent toward the surface, without a long-lasting stagnation period in intermediate crustal magmatic chambers, as proven by the presence of primary garnet bearing rocks, or by the sporadic occurrence of cognate enclaves. This is the case of Parva, Sturzii-Bucnitori, Pleşii-Mal, Oala and Iliuţa Intrusive Units, which form small intrusive bodies. An exception is Heniu Intrusive Unit, which may have paused in the upper/middle crust where it experienced an AEC process. Within this series, the decreasing of the $\delta^{18}\text{O}$ values as $^{87}\text{Sr}/^{86}\text{Sr}$ ratios and SiO_2 increase is interpreted as a progressive contamination of a mantle derived magma with a contaminant depleted in $\delta^{18}\text{O}$ and enriched in $^{87}\text{Sr}/^{86}\text{Sr}$ (i.e. hydrothermally altered lower crustal rocks).

The *high-K series* has been emplaced later in the evolution of the magmatic activity (~9 Ma). The evolution of these magmas was more complex; thus, the presence of intermediate magma chambers needs to be considered. The magmas of the Cornii and Valea Vinului Intrusive Units stagnated in large chambers (see the large volume of the intrusions) where AFC processes took place. These rocks are well crystallized, have high K and Sr content, as well as higher $^{87}\text{Sr}/^{86}\text{Sr}$ and $^{18}\text{O}/^{16}\text{O}$ ratios. The higher $\delta^{18}\text{O}$ values and $^{87}\text{Sr}/^{86}\text{Sr}$ ratios displayed by Cornii and Colibita Intrusive Units are consistent with assimilation of a different contaminant from that involved in petrogenesis of the medium-K series. This could be the local upper-crustal schists. The Măguri Intrusive Units are the youngest rocks in the area. They show characteristics of a hydrothermal system: oxygen isotope disequilibrium between coexisting pyroxenes and amphiboles, both in host-rocks and cognate enclaves, as well as additional mineralogical and petrographical alteration effects.

Acknowledgments: Special thanks are addressed to Prof. G. Cavarretta who made it possible that an important part of the present study was carried out at the CNR — Centro di Studio per il Quaternario e l'Evolutione Ambientale, Rome, within the No. 52 NATO Fellowships Programme of which D.C. Papp benefited. Laboratory managers and staff are thanked for their help during analytical work: Prof. M. Barbieri for carrying out strontium isotope analyses, A.M. Conte for the XRF measurements, M. Serracino for technical assistance during microprobe determinations and Prof. B. Turi for providing access to oxygen isotope facility. M.L. Frezzotti and F. Tecce are thanked as well for their invaluable help at various stages of this work. The authors thank Dr. J. Lexa and Dr. M. Munteanu for the critical reviewing of the manuscript.

References

- Balintoni I. 1996: Alpine structural outline of the Pannonian-Carpathian realm. *Stud. Univ. Babes-Bolyai, Geol.*, XL, 1, 55–72.
- Csontos L. 1995: Tertiary tectonic evolution of the Inter-Carpathian area: a review. *Acta Vulcanol.* 7, 1–14.
- Day R.A., Green T.H. & Smith I.E.M. 1992: The origin and significance of garnet phenocrysts and garnet-bearing xenoliths in Miocene calc-alkaline volcanics from Northland, New Zealand. *J. Petrology* 33, 125–161.
- Dobosi G., Kempton P., Downes H., Embey-Isztin A., Thirlwall M. & Greenwood P. 2003: Lower crustal granulite xenoliths from the Pannonian Basin, Hungary. Part 2: Sr–Nd–Pb–Hf and O isotope evidence for formation of continental lower crust by tectonic emplacement of oceanic crust. *Contr. Mineral. Petrology* 144, 671–68.
- Downes H., Pantó Gy., Póka T., Matthey D.P. & Greenwood P.B. 1995: Calc-alkaline volcanics of the Inner Carpathian arc, Northern Hungary: new geochemical and oxygen isotopic results. *Acta Vulcanol.* 7, 29–41.
- Eiler J.M. 2001: Oxygen isotope variation of basaltic lavas and upper mantle rocks. In: Valley J.W. & Cole D.R. (Eds.): Stable isotope geochemistry. *Rev. Mineral. Geochem.* 43, 319–364.
- Green T.H. 1992: Experimental phase equilibrium studies of garnet-bearing I-type volcanics and high-level intrusives from Northland, New Zealand. *Trans. Roy. Soc. Edinb. Earth Sci.* 83, 429–438.
- Harangi Sz., Downes H., Kosa L., Szabo Cs., Thirlwall M.F., Mason P. & Matthey D. 2001: Almandine garnet in calc-alkaline volcanic rocks of the Northern Pannonian Basin (Eastern-Central Europe): geochemistry, petrogenesis and geodynamic interpretations. *J. Petrology* 42, 1813–1843.
- Hildreth W. & Moorbath S. 1988: Crustal contribution to arc magmatism in the Andes of Central Chile. *Contr. Mineral. Petrology* 98, 455–489.
- Hoefs J. 1997: Stable isotope geochemistry. *Springer-Verlag*, Berlin, 1–201.
- Hupert H.E. & Sparks R.S.J. 1985: Cooling and contamination of mafic and ultramafic magmas during ascent through the continental crust. *Earth Planet. Sci. Lett.* 74, 371–386.
- Johnson M.C. & Rutherford M.J. 1989: Experimental calibration of the aluminium-in-hornblende geobarometer with application to Long Valley Caldera (California) volcanic rocks. *Geology* 17, 837–841.
- Kempton P.D., Downes H. & Embey-Isztin A. 1997: Mafic granulites in Neogene alkali basalts from Western Pannonian Basin: insight into the lower crust of collapsed orogen. *J. Petrology* 38, 7, 940–969.
- Leake B.E., Woolley A.R., Arps C.E.S., Birch W.D., Gilbert M.C., Grice J.D., Hawthorne F.C., Kato A., Kisch H.J., Krivovichev V.G., Linthout K., Laird J., Mandarino J.A., Maresch W.V., Nickel E.H., Rock N.M.S., Schumacher J.C., Smith D.C., Stephenson N.C.N., Ungaretti L., Whittaker J.W. & Youzhi G. 1997: Nomenclature of amphiboles: report of the Subcommittee on Amphiboles of the International Mineralogical Association, Commission on New Minerals and Mineral Names. *Amer. Mineral.* 82, 1919–1037.
- LeMaitre R.W. 1989: A classification of igneous rocks and glossary of terms. *Blackwell*, Oxford, 1–193.
- Ludwig K.R. 1994: Analyst version 2.20: a computer program for control of a thermal-ionization, single collector mass-spectrometer. *U.S. Department of Interior Geological Survey, Open File Report*, 92–543.
- Mason P., Downes H., Thirlwall M., Seghedi I., Szakács A., Lowry D. & Matthey D. 1996: Crustal assimilation as a major petrogenetic process in the East Carpathian Neogene and Quaternary continental margin arc, Romania. *J. Petrology* 37, 4, 927–959.
- Mason P.R.D., Seghedi I., Szakács A. & Downes H. 1998: Magmatic constraints on geodynamic models of subduction in the Eastern Carpathians, Romania. *Tectonophysics* 29, 157–176.
- Matthey D. & McPhearson C. 1993: High-precision oxygen isotope microanalysis of ferromagnesian minerals by laser fluorination. *Chem. Geol.* 105, 305–318.
- Matthey D., Lowry D. & McPhearson C. 1994: Oxygen isotope composition of mantle peridotite. *Earth Planet. Sci. Lett.* 128, 231–241.

- Nițoi E., Marincea Ș. & Ureche I. 1995: Enclaves in the Neogene calc-alkaline rocks in the subvolcanic zone of the East Carpathians: origin and significance. *Roman. J. Mineral.* 77, Suppl. 1, 33–34.
- Nițoi E., Munteanu M., Marincea Ș. & Paraschivoiu V. 2002: Magma-enclaves interaction in the East Carpathian subvolcanic zone, Romania: petrogenetic implication. *J. Volcanol. Geoth. Res.* 118, 229–259.
- Papp D.C. 1999: Application of stable isotopes to Earth Science. Hydrogen Isotope Geochemistry in the Rodna and Bârgău Mountains. *Ph.D. Thesis, "Babeș-Bolyai" Univ., Cluj-Napoca* 1–225 (in Romanian, with English abstract).
- Papp D.C., Tecce F., Frezzotti M.L. & Ureche I. 2003: Microthermometric study of fluid inclusions in Neogene shallow intrusions from Inner Carpathian arc (Romania). *J. Geochem. Expl.* 78–79, 105–109.
- Pécskay Z., Edelstein O., Seghedi I., Szakács A., Kovacs M., Crihan M. & Bernad A. 1995: K-Ar datings of Neogene volcanic rocks of the Neogene-Quaternary calc-alkaline volcanic rocks in Romania. *Acta Vulcanol.* 7, 53–61.
- Rădulescu D. & Săndulescu M. 1976: The plate-tectonic concept and the geological structure of the Carpathians. *Tectonophysics* 16, 155–161.
- Salter V.J.M., Hart S.R. & Pantó Gy. 1988: Origin of Late Cenozoic volcanic rocks of the Carpathian arc, Hungary. In: L. Royden & F. Horvath (Eds.): *The Pannonian Basin: a study in Basin evolution. AAPG Memoir* 45, 279–292.
- Săndulescu M. 1984: Geotectonics of Romania. *Ed. Tehn., București*, 1–336 (in Romanian).
- Seghedi I., Szakács A. & Mason P.R.D. 1995: Petrogenesis and magmatic evolution in the East Carpathians Neogene volcanic arc (Romania). *Acta Vulcanol.* 7, 135–143.
- Seghedi I., Balintoni I. & Szakács A. 1998: Interplay of tectonics and Neogene post-collisional magmatism in the Intra-Carpathian region. *Lithos* 45, 483–497.
- Seghedi I., Downes H., Pécskay Z., Thirlwall M.F., Szakács A., Prichodko M. & Matthey D. 2001: Magma genesis in a subduction-related post-collisional volcanic arc segment: The Ukrainian Carpathians. *Lithos* 57, 237–262.
- Sun S.S. & McDonough W.F. 1989: Chemical and isotopic systematics of oceanic basalts: implication for mantle composition and processes. In: Saunders A.D. & Norry M.J. (Eds.): *Magma-tism in the Ocean Basin. Geol. Soc. London, Spec. Publ.* 42, 313–345.
- Taylor H.P. Jr. 1974: The applications of oxygen and hydrogen isotope studies to problem of hydrothermal alteration and ore deposition. *Econ. Geol.* 69, 843–883.
- Thirlwall M.F., Jenkins C., Vroon P.Z. & Matthey D.P. 1997: Crustal interaction during construction of ocean islands: Pb-Sr-Nd-O isotope geochemistry of the shield basalts of Grand Canaria. *Chem. Geol.* 135, 233–262.
- Ureche I., Papp D.C. & Nițoi E. 1995: Neogene magmatites from the Rodna and Bârgău Mountains (East Carpathians): Some petrographical and petrochemical peculiarities. *Roman. J. Mineral.* 77, Suppl. 1, 56–57.
- Ureche I. 2000: Petrology of the Neogene magmatites from the Bârgău Mountains. *Ph.D. Thesis, "Babeș-Bolyai" Univ., Cluj-Napoca* 1–70 (in Romanian, with English abstract).
- Wilson M. 1989: *Igneous Petrology*. Wiley, London, 1–466.
- Zheng Y.F. 1993a: Calculation of oxygen isotope fractionation in anhydrous silicate minerals. *Geochim. Cosmochim. Acta* 57, 1079–1091.
- Zheng Y.F. 1993b: Calculation of oxygen isotope fractionation in hydroxyl-bearing silicates. *Earth Planet. Sci. Lett.* 120, 247–263.